Digest Journal of Nanomaterials and Biostructures Vol. 10, No. 4, October – December 2015, p. 1257 - 1265

STUDY OF THE LEAKAGE CURRENT IN EPITAXIAL FERROELECTRIC $Pb(Zr_{0.52}Ti_{0.48})O_3$ LAYER WITH $SrRuO_3$ BOTTOM ELECTRODE AND DIFFERENT METALS AS TOP CONTACTS

A.G. BONI[a,b*], C. CHIRILA[a], L. HRIB[a], I. PINTILIE[a], L. PINTILIE[a]
[a]*National Institute of Materials Physics, Atomistilor 105 bis, Magurele, Ilfov county, 077125, Romania*
[b]*University of Bucharest, Faculty of Physics, Magurele 077125, Romania*

The leakage current was studies in epitaxial ferroelectric $Pb(Zr_{0.52}Ti_{0.48})O_3$ layer with common $SrRuO_3$ bottom electrode and different metals as top contacts ($SrRuO_3$, Pt, Ir, Ru). It was found that the dominant conduction mechanism in the 200-350 K temperature range and for voltages significantly larger than the coercive value is the thermionic emission governed by the Schottky-Simmons equation. The height of the potential barriers was estimated and was found that this is about the same for negative and positive voltage polarities. No correlation was found between the height of the potential barriers for different top contacts and the work function difference between the bottom and top electrodes. The results suggest that the potential barrier is controlled by the polarization charges in a similar way to the one reported for $Pb(Zr_{0.2}Ti_{0.8})O_3$ and $BaTiO_3$ epitaxial films with bottom $SrRuO_3$ electrode and different metals as top contacts. It was also found that above 350 K the conduction mechanism changes to ohmic and/or space charge limited currents.

(Received September 15, 2015; Accepted November 9, 2015)

Keywords: epitaxial, $Pb(Zr_{0.52}Ti_{0.48})O_3$, conduction mechanisms

1. Introduction

Ferroelectric materials are attractive for a large variety of applications due to their special proprieties such as spontaneous polarization, pyroelectric, photovoltaic and piezoelectric effects, and non-linear optical properties. [1], [2]. In many of these applications the ferroelectric materials are used in capacitor-like configurations, and the working principle implies the application of an external electrical voltage [1], [3], [4]. Besides the very good dielectric and ferroelectric proprieties there is also a damaging parameter, namely the magnitude of the leakage current. The control of the leakage current is especially important in ferroelectric capacitors used for non-volatile memories because it is believed to be linked to the rapid time dependent destruction of the information stored in the memory devices [5]. This represents a strong motivation for a large number of research groups to study the conduction mechanisms responsible for the leakage current in ferroelectric capacitors [1].

Even if the main response of a ferroelectric capacitor to an applied voltage consists in a change of polarization, the leakage current through the ferroelectric thin films can have noticeable values due to the large electrical field ($10^4 - 10^5 \frac{V}{cm}$ even for a few applied volts) and due to the finite resistance of the material. The first studies of the leakage current in ferroelectric thin films have been performed on polycrystalline or defective layers. In these cases the current magnitude depends on stoichiometry, deposition temperature, annealing temperature, electrode material, and microstructure. This variety of factors leads to different interpretation of data, using different transport models. The conduction mechanisms which are responsible for the charge transport through a thin films have been divided in two major categories: those that depend on the electrical

Corresponding author:* andra.boni@infim.ro

properties of the electrode-ferroelectric interface, which are called electrode-limited (thermionic emission, thermionic-field emission, tunneling), and those that depend only on the properties of the material, which are called bulk-limited (Pool-Frenkel emission, hopping, ohmic, space-charge-limited currents) [6]–[9].

The evolution of synthesis and deposition methods of thin films allow to obtain epitaxial layers with very good quality of structure and interfaces [10]. For these systems, the leakage currents has an increased values compared with polycrystalline films, the high resistivity of the latter cases being attributed to extrinsic contribution as grain boundaries, dislocations and domain walls which can act as trapping or scattering centers for mobile charges, leading to reduction of charge density and mobility [11]. For epitaxial thin films, the leakage current has been explained especially by electrode injection mechanisms (thermionic emission [12] or tunneling [13]), or by a transport mechanism which combines electrode injection with drift-diffusion in the film bulk [14]. Thus, for explaining the dependence of the leakage current on voltage and temperature in the case of high quality epitaxial ferroelectric thin films, the Schottky-Simmons equation is most used [15], [16]. It was already shown that the electrode interfaces can significantly affect the macroscopic electrical properties of ferroelectric capacitors such as dielectric constant and polarization switching [17], [18]. However, in [17] it has been shown, for two different ferroelectric materials with tetragonal structure ($Pb(Zr_{02.}Ti_{0.8})O_3$-PZT and $BaTiO_3$), that the potential barriers obtained for different top electrodes are about the same even if there are significantly differences in work functions, leading to the conclusion that the ferroelectric polarization is actually controlling the height of the potential barrier.

The effect of the electrode interfaces on the leakage current in epitaxial PZT films with composition near the morphotropic phase boundary and deposited on $SrTiO_3$ (STO) buffered Si wafers were less studied. In this work we analyze the leakage current for PZT films with Zr/Ti ratio of 52/48 grown by pulsed laser deposition (PLD) on a $STO/SiO_2/Si$ substrate. The STO buffer layer was grown by MBE, then a bottom $SrRuO_3$ (SRO) electrode has been deposited by PLD. Several metals were then used as top electrodes of the capacitor-like structures: Pt, Ir, Ru, and SRO.

2. Experimental methods

The growth details of STO on Si (001) can be found in [19], [20]. SRO bottom electrode and PZT ferroelectric layer were deposited by PLD, using a KrF pulsed excimer laser with a wavelength of 248 nm, as it is described in [21]. The ablation process of PZT was carried out at a laser fluence of 2 J/cm^2 and a repetition rate of 5 Hz, for 10 000 pulses, in an oxygen atmosphere of 20 Pa. After deposition the film was annealed for 1h in 10^5 Pa O_2 pressure, and then cooled down at room temperature. The capacitor structures were obtained by the deposition of 100x100 μm^2 area top electrodes using a shadow mask. Different metals were used as top contacts: SRO ($\phi_{SRO} = 4.6 - 4.9$ eV), Pt ($\phi_{Pt} = 5.65$ eV), Ir ($\phi_{Ir} = 5.67 - 5.72$ eV) and Ru ($\phi_{Ru} = 4.71$ eV) [22]–[24]. SRO was deposited by PLD at room temperature, while Pt, Ir and Ru were deposited by radio-frequency (RF) sputtering.

Details about structure can be found in previous paper [21], and it was found that the STO, SRO and PZT layers grow epitaxial on the Si (001) substrate. Therefore the electrical properties (especially leakage currents) are not affected by extrinsic contributions (for example grain boundaries).

The current-voltage (I-V) characteristics were measured by using a Keithley 6517 electrometer with an incorporated dc voltage source. The temperature measurements were performed by introducing the samples into a Lake Shore cryoprober model CPX-VF with CuBe needles. The data acquisition was automatic, special software being developed for this type of measurements.

Before presenting and discussing the experimental data one has to describe in more details how the I-V measurements were performed. The standard procedure is to raise the DC voltage in small steps, to wait a certain period of time until the DC leakage current is stabilized and then to record the current value. In the present case the voltage steps were of 200 mV, the waiting time

was set to 1 second and the current value recorded in the I-V measurement is an average over 5 readings. The time necessary for communications between computer and the measuring instrument and the time for averaging the current add to the waiting time leading the total time between two points in the I-V characteristic to about 3 seconds. From current-time (I-t) measurements was found that this time is sufficient to have a stable current value for voltage range where the polarization is saturated. At smaller voltages, in between the values corresponding to the coercive field, the current is altered by contributions related to polarization back-switching. This fact is visible especially at low temperature, probably due to a slow compensation process of the depolarization field [25], [26].Elimination of the back-switching contribution at low temperatures would have required waiting times of the order of 10 seconds. The problem is that long waiting times can lead to time-dependent breakdown of the ferroelectric capacitor because of lengthy exposure to DC voltages [27], [28]. Breakdown would have made meaningless the current measurements as long as are not performed on the same capacitor for the entire temperature range. In order to find the voltage ranges where the parasitic contributions from polarization switching are negligible, static hysteresis was measured and compared with the current hysteresis measured in similar conditions (see Fig. 1(a)). The dynamic polarization and current hysteresis were also recorded at a frequency of 1 kHz (see Fig. 1(b)).

Details about the dynamic and static hysteresis measurement can be found in [29]. The difference between the measurements is that the dynamic hysteresis is obtained by continuous integration of the current flowing through the ferroelectric capacitor when the triangular voltage is varied between $-V_{max}$ and $+V_{max}$ with a certain frequency (1 kHz in the present case), while the static hysteresis is obtained point-by-point in quasi-static conditions. One can say that a relaxed polarization is recorded in the static hysteresis. This is the reason why the polarization saturation is better seen in the static hysteresis. Regarding Fig. 1(a), it can be seen that at voltages higher than -6 V for negative polarity and +6 V for positive polarity the non-linear ferroelectric polarization is saturated and is no longer bringing parasitic contribution to the leakage current when the voltage is swept down. Therefore, only the values recorded while sweeping down the voltage were considered for further analysis. In this way polarization orientation is set during the voltage sweeping up and does not change while sweeping down the voltage in the range outside the marked box in Fig. 1(a). Repeating same types of measurements at different temperatures and for different top contacts it was found that the I-V characteristics recorded above 200 K, with a waiting time of 1 second and a total time between to current reading of 3 seconds, are not affected by polarization switching currents at voltages higher than: -3/+3 V for top SRO contacts; -6/+6 V for top Ir and Pt contacts; -6 V for top Ru contact (for positive polarity it was not possible to extract meaningful information). It was also found that breakdown is possible for temperatures above 350 K. Therefore, only the data recorded between 200 K and 350 K, in the above mentioned voltage ranges, were used for extracting information on the conduction mechanism responsible for the leakage current. It has to be mentioned that epitaxial ferroelectrics, as it is the case, are considered wide gap semiconductors rather than dielectrics thus the leakage current can have significant values [30]–[32].

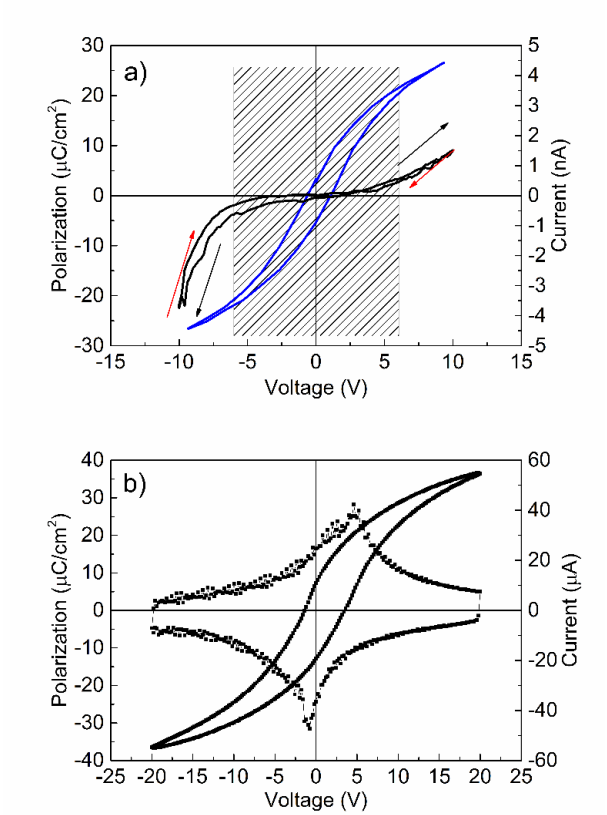

Fig. 1 a) Static hysteresis recorded with a delay time of 1 second, and the current hysteresis recorded with a waiting time of 1 second. The arrows indicate the voltage sweep up and down. Only the down current readings were considered for further analysis. The marked area between -6 V and +6 V indicates the voltage domain were the current is still affected by parasitic contributions from the polarization switching. b) Dynamic hysteresis recorded with a triangular voltage wave of 1 kHz. Measurements were performed at room temperature, on top Ir contact. Similar results are obtained on the other contacts.

3. Results and discussions

The current-voltage measurements were performed from 150 K to 400 K with a step of 10 K. The I-V characteristics for the four different top contacts are presented in Fig. 2.

There can be seen that the different top electrodes show different voltage and temperature dependencies of the current. For example structure with SRO as top electrodes has symmetrical current-voltage characteristics, with a weak dependence on temperature in 150 K-330 K range.

Structures with Pt and Ir as top electrode have current-voltage characteristic with a strong dependence on temperature. At low temperatures the loop is not symmetrical, but at temperatures greater than 300 K the current becomes symmetrical with respect to voltage. For Ru electrodes it can be seen that the current has a strong asymmetry, with greater values for negative polarity which also has obvious temperature dependence, while for positive polarity currents are lower and with less pronounced temperature dependence.

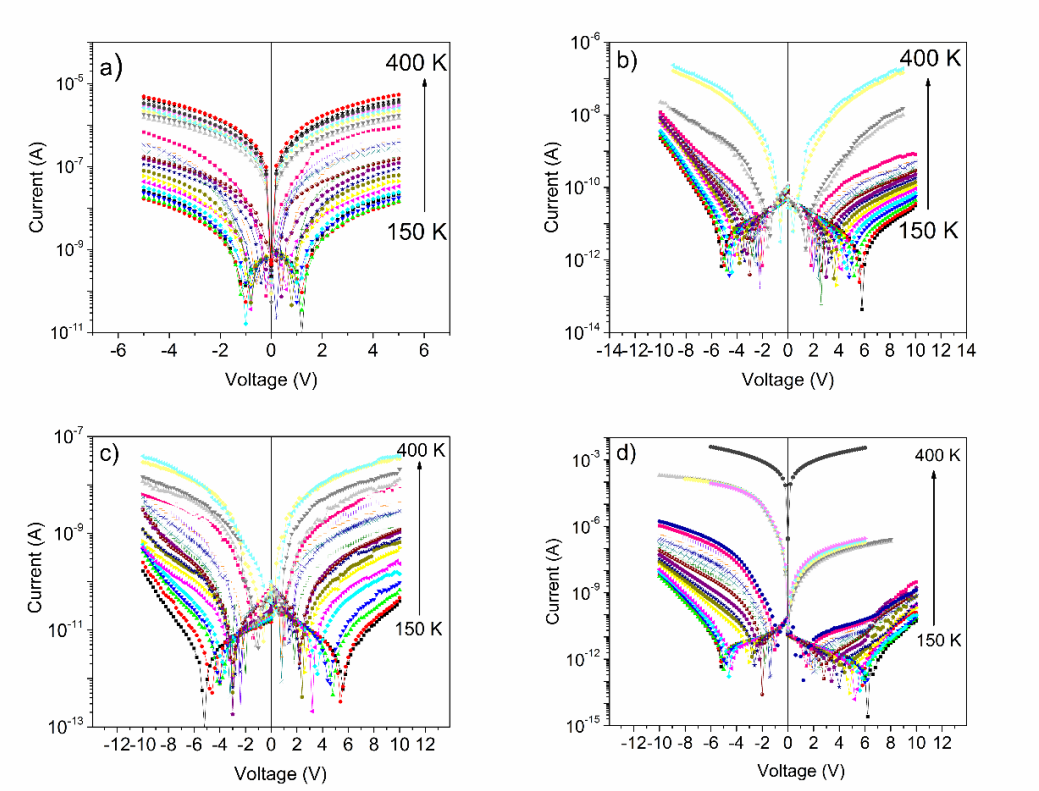

Fig.2 I-V characteristics for epitaxial PZT thin films deposited on Si substrates with different top electrodes. The characteristics were recorded in the 150–400 K temperature range for: a) SRO top electrode , b) Pt top electrode, c) Ir top electrode and d) Ru top electrode.

For further analysis regarding the conduction mechanism only the I-V data in the temperature range from 200 K to 350 K will be considered. At temperatures below 200 K the contribution from polarization switching is still significant even at voltage as high as -7/+7 V, leaving only a small voltage range where the leakage current is not affected by parasitic contributions. For temperatures above 200 K the voltage ranges where the leakage current is not affected by the polarization switching contributions were selected according to procedure described in section

The I-V characteristics where analyzed assuming the presence of the Schottky-type contacts at the electrode interfaces, as previous results suggested [21]. Therefore, Schottky emission over the potential barrier was assumed as dominant conduction mechanism. Taking into account that the mean free path of charges in ferroelectrics is much smaller than the film thickness, a general Schottky-Simmons equation [16], [33] was used to explain the voltage and temperature dependence of the current:

$$J = 2q\left(\frac{2\pi m_{eff} kT}{h^2}\right)^{3/2} \mu E \exp\left(-\frac{q}{kT}\left(\phi_B^0 - \sqrt{\frac{qE_m}{4\pi\varepsilon_0\varepsilon_{op}}}\right)\right) \quad (1)$$

Here J is the current density, q is the electron charge, h is the Planck's constant, m_{eff} is the effective mass, μ is the mobility, k is the Boltzmann's constant, T is the temperature, E is the electrical field

in the film, ε_0 is the vacuum permittivity, ε_{op} is the optical dielectric constant, ϕ_b^0 is the interfacial potential barrier height at 0V, and E_m is electrical field at the interface.

The values obtained for ε_{op} at 300K, using the $\ln(J/E) = f(E^{1/2})$ representation for SRO, Pt, Ir, Ru top electrodes, are: 4.23, 5.58, 5.05, 4.36 (see Table 1). These are comparable with the values reported in literature, were ε_{op} is around 5-6.5 for PZT [34]. Therefore we can assume that the conduction mechanism responsible for the leakage current in this cases is the thermionic injection controlled by the electrode interfaces followed by the drift-diffusion controlled by the bulk as described by equation 1.

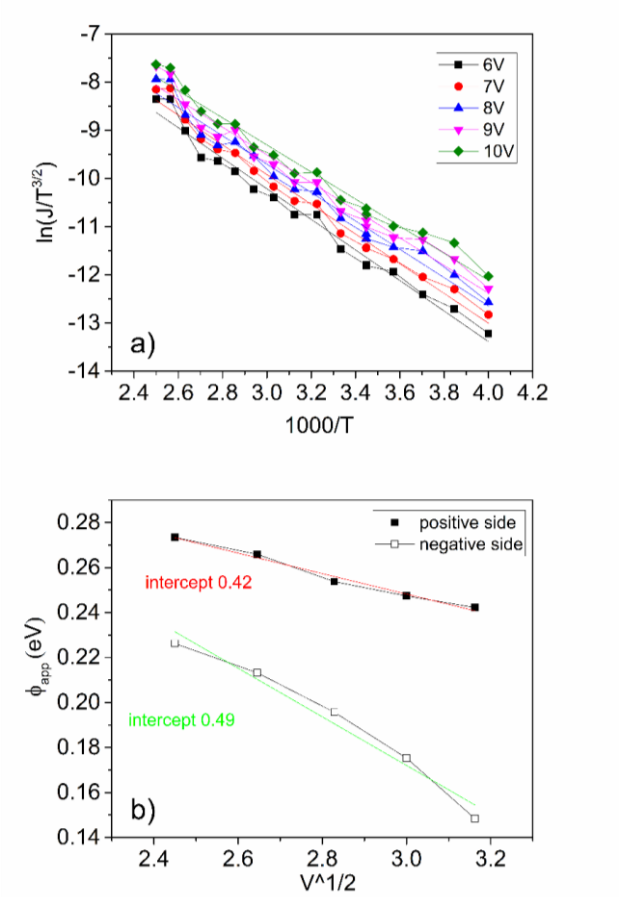

Fig.3 a) Arrhenius representation for positive polarity for Ir electrode; b) the apparent potential barrier dependence on $V^{1/2}$.

The slopes of the Arrhenius representation $\ln(J/T^{3/2}) = f(1000/T)$, shown in Fig. 3(a) for positive polarities in the case of Ir top electrode, give the apparent potential barrier [16]. It has been shown that the apparent potential barrier has a linear dependence on the square root of the applied voltage thus, by extrapolating the $\phi_{app} = f(V^{1/2})$ representation to 0V one can obtain the value ϕ_B^0 of the potential barrier ay zero volts (see Fig. 3(b)).

Following this procedure, the potential barriers were calculated for top SRO, Pt, Ir and Ru contacts. The corresponding values are given in Table 1. One can see that the values for positive and negative voltage polarities on the top electrodes, corresponding to reverse biasing of the two electrode interfaces, are very similar although the difference in work functions can be significant (up to 1 eV for bottom SRO and top Ir or Pt). One cannot say which interface is reverse biased for positive voltage and which for negative one because it is not clear if the PZT layer is *n* or *p* type. However, considering that the two interfaces act as back-to-back Schottky diodes, then one of the electrode interfaces is reversed biased no matter the polarity of the applied voltage [35]. Another

observation is that the height of the potential barriers does not depend on the polarity of the applied voltage. This result is expected for symmetrical structure, where both electrodes are SRO, but one would expect that for one polarity, the barrier height to change when top electrode is different from the bottom one. This result can be explained as in ref. [17], assuming that the polarization charges are controlling the height of the potential barrier at the electrode-ferroelectric interface. On the other side, there is a significant difference between the height of the potential barrier obtained for SRO on one hand, and the metallic electrodes as Pt and Ir on the other hand. As in [36]–[38], there is expected to have an increased leakage current and a lower barrier height for oxide electrodes (SRO), due to a significant concentration of oxygen vacancies in the PZT layer.

One has to mention also that the potential barrier for positive polarity on Ru could not be estimated due to large current fluctuations leading to contact breakdown. Also it can be noted that the potential value for Ru electrode is between SRO and Pt or Ir. This fact could be explained if consider that Ru can oxides, forming RuO_2 at the interface with PZT by taking the necessary oxygen from the PZT film.

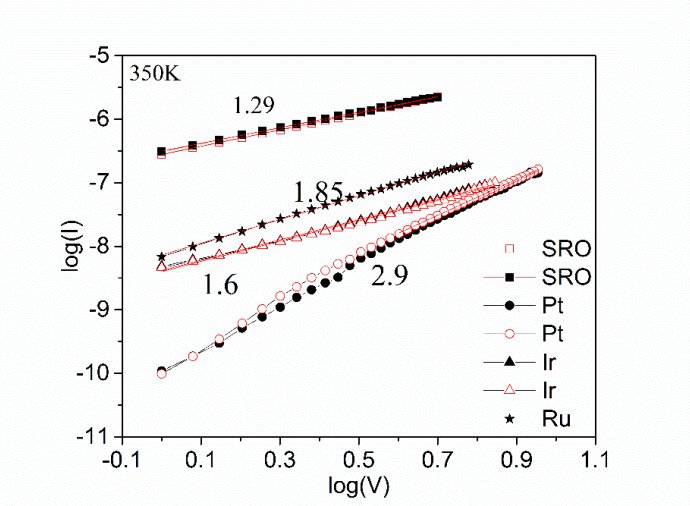

Fig.4 Linear dependence of log(I) as function of log(V) representation at 350K, with 1.29, 2.9, 1.6 and 1.85 values of slopes for SRO, Pt, Ir, Ru electrodes

For temperatures greater than 350K, the IV curves become symmetrical and the leakage current has an almost linear or quadratic dependence on voltage, as shown in Fig. 4. This suggests a change in the conduction mechanism towards a bulk controlled one, which can be ohmic conduction or/and space charge limited currents (SCLC). It seems that at elevated temperatures the potential barriers becomes "transparent" to charge carrier injection, acting as quasi-ohmic contacts.

Table 1. The values of the potential barriers height (ϕ_B^0(eV)), calculated for negative and positive polarities of the voltage applied on the top electrodes made from different metals. The optical dielectric constant (ε_0) is also given, as estimated from the slope of $\ln(J/E) = f(E^{1/2})$ *representation (see further in the text).*

Electrode	ε_{op}	Φ_B^0**(eV)**	
		Positive	Negative
SRO	4.23	0.12	0.11
Pt	5.58	0.43	0.47
Ir	5.05	0.42	0.49
Ru	4.36	-	0.24

4. Conclusions

We present the effect of the top electrode interface on the leakage current in ferroelectric capacitors based on $PbZr_{0.52}Ti_{0.48}O_3$ films deposited on Si substrate with STO as a buffer layer. The bottom electrode was SRO and four different metals were used as top contacts: SRO, Pt, Ir, and Ru.

The dominant conduction mechanism was assumed to be Schottky emission, in line with the presence of the Schottky type contacts at the electrode interfaces. The analysis of the experimental data has revealed that the potential barriers do not correlate with the work function values of the metals used as top electrodes. It was found that for Pt and Ir top electrodes the potential barriers for positive and negative polarities are about the same although the bottom SRO electrode has a lower work function. In the case of SRO, the leakage current is higher and potential barrier is lower than for metallic electrodes. The Ru top electrodes has a behavior between Pt/Ir and SRO. At high temperatures the conduction mechanism seems to change from Schottky emission to space charge limited currents.

Acknowledgements

The authors acknowledge the financial support of the Romanian Ministry of Education-Executive Unit for Funding High Education, Research, Development and Innovation (MEN-UEFISCDI) through the Idea-Complex Research Grant PN-II-ID-PCCE-2011-2-0006 (contract nr. 3/2012). The authors wish to thank to S. Yin from CEA LETI Minatec Campus 17, rue des Martyrs 38054 Grenoble, France for depositing the Ru top electrodes. The authors wish to thank also to Guillaume Saint-Girons, G. Niu and Y. Robach from Institute des Nanotechnologies de Lyon Ecole Centrale de Lyon 36, Avenue Guy de Collongue 69134 Ecully, France for providing the Si substrates with the STO buffer layer deposited by MBE. Andra Georgia Boni thanks to the strategic grant POSDRU/159/1.5/S/137750, "Project Doctoral and Postdoctoral programs support for increased competitiveness in Exact Sciences research" cofinanced by the European Social Found within the Sectorial Operational Program Human Resources Development 2007-2013.

References

[1] J. F. Scott, Ferroelectric Memories vol. 3, Berlin, Heidelberg, Springer Berlin Heidelberg (2000).
[2] K. M. Rabe, C. H. Ahn, J.-M. Triscone, Physics of Ferroelectrics: A Modern Perspective, Springer Science & Business Media (2007).
[3] K. Uchino, Ferroelectric Devices, CRC Press (2000).
[4] M. E. Lines, A. M. Glass, Principles and Applications of Ferroelectrics and Related Materials, Oxford University Press (2001).
[5] T. P. Ma, J.-P. Han, IEEE Electron Device Lett. **23**(7), 386 (2002).
[6] J. G. Simmons, J. Phys. Appl. Phys. 4(5), 613 (1971).
[7] K.-C. Kao, W. Hwang, Electrical transport in solids: with particular reference to organic semiconductors, Pergamon Press (1981).
[8] K.-C. Kao, Dielectric Phenomena in Solids: With Emphasis on Physical Concepts of Electronic Processes, Academic Press (2004).
[9] S. M. Sze, Physics of Semiconductor Devices, 2nd edition. John Wiley & Sons (1981).
[10] L. W. Martin, Y.-H. Chu, R. Ramesh, Mater. Sci. Eng. R Rep. **68**(4–6), 89 (2010).
[11] I. Vrejoiu, G. Le Rhun, L. Pintilie, D. Hesse, M. Alexe, U. Gösele, Adv. Mater. **18(**13), 1657 (2006).
[12] C. S. Hwang, B. T. Lee, C. S. Kang, J. W. Kim, K. H. Lee, H.-J. Cho, H. Horii, W. D. Kim, S. I. Lee, Y. B. Roh, M. Y. Lee, J. Appl. Phys. **83**(7), 3703 (1998).
[13] J. C. Shin, J. Park, C. S. Hwang, H. J. Kim, J. Appl. Phys. **86(**1), 506 (1999).
[14] H. Schroeder, S. Schmitz, P. Meuffels, Appl. Phys. Lett. **82**, 5 (2003).

[15] J. G. Simmons, Phys. Rev. Lett. **15(**25), 967 (1965).
[16] L. Pintilie, I. Vrejoiu, D. Hesse, G. LeRhun, M. Alexe, Phys. Rev. B **75**(10), 104103 (2007).
[17] I. Pintilie, C. M. Teodorescu, C. Ghica, C. Chirila, A. G. Boni, L. Hrib, I. Pasuk, R. Negrea, N. Apostol, L. Pintilie, ACS Appl. Mater. Interfaces **6(**4), 2929 (2014).
[18] L. Pintilie, I. Vrejoiu, D. Hesse, M. Alexe, J. Appl. Phys. **104(**11), 114101 (2008).
[19] G. Niu, G. Saint-Girons, B. Vilquin, G. Delhaye, J.-L. Maurice, C. Botella, Y. Robach, G. Hollinger, Appl. Phys. Lett. **95(**6), 062902 (2009).
[20] G. Niu, J. Penuelas, L. Largeau, B. Vilquin, J. L. Maurice, C. Botella, G. Hollinger, G. Saint-Girons, Phys. Rev. B **83**(5), 054105 (2011).
[21] C. Chirila, A. G. Boni, I. Pasuk, R. Negrea, L. Trupina, G. L. Rhun, S. Yin, B. Vilquin, I. Pintilie, L. Pintilie, J. Mater. Sci. **50(**11), 3883 (2015).
[22] A. J. Hartmann, M. Neilson, R. N. Lamb, K. Watanabe, J. F. Scott, Appl. Phys. A **70(**2), 239 (2000).
[23] J. K. Schaeffer, L. R. C. Fonseca, S. B. Samavedam, Y. Liang, P. J. Tobin, B. E. White, Appl. Phys. Lett. **85**, 10 (2004).
[24] H. B. Michaelson, J. Appl. Phys. **48(**11), 4729 (1977).
[25] B. Peng, Z. Xie, Z. Yue, L. Li, J. Appl. Phys. **116**(3), 034109 (2014).
[26] T. K. Song, Y. W. So, D. J. Kim, J. Y. Jo, T. W. Noh, Integr. Ferroelectr. **73(**1), 115 (2005).
[27] I. Stolichnov, A. Tagantsev, J. Appl. Phys. **84(**6), 3216 (1998).
[28] E. Bouyssou, R. Jérisian, N. Cézac, P. Leduc, G. Guégan, C. Anceau, Mater. Sci. Eng. B **118(**1–3), 28 (2005).
[29] L. Pintilie, I. Pasuk, R. Negrea, L. D. Filip, I. Pintilie, J. Appl. Phys. **112(**6), 064116 (2012).
[30] J. F. Scott, Science **315(**5814), 954 (2007).
[31] H. Matsuura, New J. Phys. **2**, 8 (2000).
[32] M. Kobune, O. Matsuura, T. Matsuzaki, A. Mineshige, S. Fujii, H. Fujisawa, M. Shimizu, H. Niu, Jpn. J. Appl. Phys. **39**(9B), 5451 (2000).
[33] B. Nagaraj, S. Aggarwal, R. Ramesh, J. Appl. Phys. **90(**1), 375 (2001).
[34] M. P. Moret, M. a. C. Devillers, K. Wörhoff, P. K. Larsen, J. Appl. Phys. **92(**1), 468 (2002).
[35] C. Ge, K. Jin, C. Wang, H. Lu, C. Wang, G. Yang, J. Appl. Phys. **111**(5), 054104 (2012).
[36] I. Stolichnov, A. Tagantsev, N. Setter, J. S. Cross, M. Tsukada, Appl. Phys. Lett. **75**(12), 1790 (1999).
[37] J. J. Lee, C. L. Thio, S. B. Desu, J. Appl. Phys. **78(**8), 5073 (1995).
[38] H. Al-Shareef, A. I. Kingon, X. Chen, K. R. Bellur, O. Auciello, J. Mater. Res. **9**(11), 2968 (1994).